Journal of Statistical Physics, Vol. 76, Nos. 1/2, 1994

Microscopic Approach to the Formation of Liesegang Patterns

Bastien Chopard,[1] Pascal Luthi,[1] and Michel Droz[2]

Received October 8, 1993; final April 1, 1994

A microscopic approach to the formation of Liesegang patterns, based on a cellular automata model, is presented. This approach gives a consistent description of several types of patterns observed experimentally (bands, rings, and spirals). Quantitative predictions are made about the generic laws (time, spacing, and width laws) governing the formation of these patterns. Emphasis is put on the role played by the fluctuations in such nonequilibrium systems.

KEY WORDS: Pattern formation; reaction-diffusion phenomena; Liesegang rings; nucleation; aggregation; cellular automata; lattice Boltzmann simulations.

1. INTRODUCTION

Reaction-diffusion-like problems have experienced in recent years a renewal of interest due to the development of several new approaches, both from the experimental and theoretical points of view. Problems of anomalous kinetics,[1,2] front formation,[3,4] and Turing patterns formation[5-7] have stimulated a vast body of work. In all these problems, a description in terms of rate (or mean-field-like) equations is not sufficient. It is important to go beyond a mean-field-like approach and take the statistical fluctuations into account. Accordingly, first-principle analytical results are scare. On the other hand, it was recently shown that cellular automata-like models[7-9] provide a powerful numerical tool to study such problems.

A very interesting class of problems concerns Liesegang patterns formation. These patterns are produced by precipitation in the wake of a moving reaction front.

[1] Parallel Computing Group, University of Geneva, CH-1211 Geneva 4, Switzerland.
[2] Department of Theoretical Physics, University of Geneva, CH-1211 Geneva 4, Switzerland.

0022-4715/94/0700-0661$07.00/0

Such a pattern formation is typically observed in a test tube containing a gel in which a chemical species B (for example, $AgNO_3$) reacts with another species A (for example, HCl). At the beginning of the experiment, B is uniformly distributed in the gel with concentration b_0. The other species A, with concentration a_0 is allowed to diffuse into the tube from its open extremity. Provided that the concentration a_0 is larger than b_0, a reaction front propagates in the tube. As this $A + B$ reaction goes on, formation of consecutive bands of precipitate (AgCl in our example) is observed in the tube (see Fig. 1a).

A striking feature is that this formation process obey simple generic laws. After a transient time, these bands appear at some positions x_i and times t_i and have a width w_i. It is first observed that the center position x_n of the nth band is related to the time t_n of its formation through the so-called time law $x_n \sim \sqrt{t_n}$. Second, the ratio $p_n \equiv x_n/x_{n-1}$ of the positions of two consecutive bands approaches a constant value p for large enough n. This last property is known as the Jablczynski law[10] or the spacing law. Finally, the width w_n of the the nth band is an increasing function of n. The presence of bands is related to the geometry of the experiment, i.e., the use of a test tube with axial symmetry, and most of the experiments have been performed in this case. However, for more complicated geometries, different shapes may be obtained. A well-known example is provided by the rings formed in agate rocks.[10-12]

It is well known that in the reaction-diffusion process described above the reaction front position $x_f(t)$ obeys the relation $x_f(t) \sim \sqrt{t}$,[13] with an amplitude depending on the difference of the concentrations a and b. This behavior is mainly a consequence of the diffusive character of the motion of the particles. As the Liesegang patterns are formed in the wake of a moving reaction front, the time law appears to be a simple consequence of the diffusive dynamic. However, spacing and width laws cannot be derived only with reaction-diffusion hypotheses. Extra nucleation-aggregation mechanisms have to be introduced, which makes any analytical derivation quite intricate.

The formation of Liesegang patterns has been investigated by many researchers, both from an experimental and a theoretical point of view. The models proposed so far belong to three categories[14]: sol coagulation models, competitive particle growth models, and supersaturation models. So far, none of these models is able to account for all experimental observations. For example, particular situations, called inverse banding,[15] where the distance between successive rings decreases as time increases, are not directly explained by these models. New ingredients expressing the capacity of the gel to dissolve the precipitates should be introduced. However, we believe, following Prager,[16] Zeldovitch *et al.*,[17] Smith,[18]

Dee,[19] and Le Van and Ross,[20] that the supersaturation mechanism based on Ostwald's ideas[21] plays a crucial role in the band formation.

Two different scenarios can then be devised. In the most recent one, proposed by Dee,[19] the two species A and B react to produce a new species C which also diffuses in the gel. This C species represents a colloidal state which is observed in several experiments.[18] When the local concentration of C reaches some threshold value, nucleation occurs: the C particles precipitate and become D particles at rest. This process is described by the equations

$$\begin{aligned} \partial_t a &= D_a \nabla^2 a - R_{ab} \\ \partial_t c &= D_c \nabla^2 b - R_{ab} \\ \partial_t c &= D_c \nabla^2 a + R_{ab} - n_c \\ \partial_t d &= n_c \end{aligned} \tag{1}$$

where a, b, c, and d stand for the concentration at time t and position $\mathbf{r}$ of the A, B, C, and D species, respectively. The term R_{ab} expresses the production of the C species due to the $A + B$ reaction. Classically, a mean-field approximation is used for this term and $R_{ab} = kab$, where k is the reaction constant. The quantity n_c describes the depletion of the C species resulting from nucleation and aggregation on existing D clusters. A precise expression for this quantity is quite complex and we will return to it in more detail later.

From Eqs. (1), the existence of bands may be understood as follows (Ostwald): due to aggregation, the droplets of nucleated D particles formed at the reaction front deplete their surroundings of the reaction product C. As a result, the level of supersaturation drops dramatically and the nucleation and solidification processes stop. After some time, the reaction front has moved away and the concentration of the C product at the moving front reaches a value large enough to allow the nucleation to occur again. As a result, separated bands will appear.

However, depending on the chemical constituent A and B, it is not clear that whether the intermediate C species exists as an individual diffusing molecule. If not, another scenario has been proposed by Prager,[16] Zeldovitch *et al.*,[17] and Smith.[18] There, the A and B species coexist in the gel until the solubility product ab reaches a critical value above which nucleation occurs according to the reaction $A + B \rightarrow AB(\text{solid})$. As nucleation has started, a depletion of A and B occurs in the surrounding and the same mechanism as described above take place to produce separated bands.

Until very recently, the above two scenarios were only investigated at the mean-field level. The Prager–Zeldovitch model has been solved analytically[18] assuming the *a priori* existence of bands. The spacing law could be established from this derivation. Dee[19] and later Le Van and Ross[20] considered numerical solutions of the partial differential equations governing the reaction-diffusion-solidification processes. The theoretical results agree qualitatively with the experimental ones for large initial concentration differences of precipitating ions and large initial degree of supersaturation. However, not enough bands have been obtained to provide a conclusive verification of the spacing law and to establish a width law.

In a recent letter[22] we showed, in the case of a simple axial geometry, that both the Prager–Zeldovitch and Dee scenarios can be considered at a microscopic level in terms of cellular automata models. One of the main advantages of this approach lies in the fact that time- and space-dependent statistical fluctuations are included. For simple reaction-diffusion systems with reaction fronts, it has been shown[3] that these fluctuations are important for a dimension $d \leqslant d_u = 2$. For aggregation mechanisms it is believed[23] that the statistical fluctuations play an important role for all dimensions. Thus, adding statistical fluctuations is an important ingredient to explain the properties of Liesegang-like patterns. Moreover, beyond the simple laws describing the patterns at the macroscopic scale, these patterns have a nontrivial mesoscopic structure. The Liesegang rings observed experimentally are not always compact, but are formed by ramified structures, which may have some fractal properties. Our approach should allow us to describe not only the macroscopic properties of the patterns, but also the microscopic ones.

The goal of this paper is to investigate in more detail the cellular automata approach we have proposed recently.[22] We show that our models are able to produce Liesegang bands satisfying the generic formation laws. In addition, more general situations can be considered and we give results of ring and spiral structures which compare qualitatively well with experimental observations. We also describe various other patterns that are obtained when different parameters are used in the simulation. We introduce a qualitative phase diagram where all these patterns are represented, with the following terminology: amorphous solidification, homogeneous clustering, Liesegang patterns, and mineral dendrite. Finally, we propose new quantitative predictions that call for experimental verification.

The paper is organized as follows. In Section 2, we introduce the cellular automata model for the situation where C particles are present. A lattice Boltzmann approximation of our rule is discussed to increase the speed of our simulations. Then the second model, without C, is introduced. In Section 3, the results for a system with axial symmetry (bands) are

reviewed and the different possible patterns emerging from the models represented in terms of a phase diagram. In Section 4, the case of two-dimensional rings and spiral formation is discussed. Finally, the importance of the fluctuations is discussed in Section 5.

2. THE MICROSCOPIC APPROACH

2.1. The Cellular Automata Model

Cellular automata models offer a powerful approach to the description of many complex systems. They consists of fully discrete universes. Particles move on a regular lattice, simultaneously, according to discrete time steps. The interactions between the particles are chosen to reflect only the essential features of the real microscopic world.

This approach amounts to solving a many-body problem as opposed to mean-field-like approaches. Moreover, cellular automata models are tailored to be implemented on a massively parallel computer, ensuring very efficient simulations.

Our model is defined on a two-dimensional square lattice. For the axial system (test tube), the initial conditions are the following: at time $t=0$, the left part of the system ($x \leqslant 0$) is randomly occupied by A particles with a density a_0 and the right part ($x>0$) is filled with B particles with a density b_0, as suggested by Fig. 1a.

The particles are restricted to move along the main directions of the lattice, according to a discrete time clock. Particles which meet at the same site interact or transform according to the rules of the cellular automaton. In the case where C particles are considered (Dee's model), four basic mechanisms are introduced in our model: (i) diffusion, (ii) reaction, (iii) spontaneous precipitation (nucleation), and (iv) aggregation.

Diffusion corresponds to a simultaneous random walk of all particles on the lattice.[24] We will use four bits at each site to represent the particles of each diffusing species. Each of these four bits describes the absence or the presence of a particle of the given species traveling in one of the four possible directions of the lattice (up, right, down, or left). Our dynamics is such that it never happens that two or more particles of a given species enter simultaneously the same lattice site in the same direction. This fact (known as an exclusion principle) guarantees that four bits are enough, in two dimensions, to describe each species at any time.

In absence of diffusion and reaction, the particles would simply move in straight lines, hopping at each time step to a neighboring site. Diffusion

is produced as follows: at each time step, the four bits representing the configuration of particles entering at each site undergo a random permutation. In practice, we simply consider a random rotation (of 0, $\pi/2$, π, or $-\pi/2$) of the lattice directions. Then the particles move to the next site of the lattice, according to their new velocity direction. In this way, the number of particles is conserved during the updating and the exclusion principle is always obeyed without having to deal with conflicting particle motions. The probabilities of each of the random rotations allow us to adjust the diffusion coefficient of each species.[24]

The production of C particles takes place according to the reaction $A+B\to C$. At the level of the cellular automata rule, this process is modeled as follows: when two particles of species A and B collide at a given site, they disappear with some given probability k and produce a C particle. This reaction is only possible if there is still room for this new C particle (the exclusion principle restricts their number to four at each site). If no reaction takes place, the two initial particles ignore each other and continue their own motion. These rules can be expressed by evolution equations which are defined as the microdynamics of the model. Let us call the four bits describing each species as $a_i(\mathbf{r}, t)$, $b_i(\mathbf{r}, t)$, and $c_i(\mathbf{r}, t)$, $i=1,\ldots, 4$. The microdynamics can be divided into two steps: the reaction phase and the diffusive motion. We denote a_i', b_i', and c_i' the quantities just after the reaction phase. For the sake of simplicity, we assume that the $A+B$ reaction takes place only when the A and B particles meet with opposite velocities:

$$\begin{aligned} a_i' &= a_i - \kappa_i a_i b_{i+2}(1-c_{i+1}) \\ b_i' &= b_i - \kappa_{i+2} a_{i+2} b_i (1-c_{i+3}) \\ c_i' &= c_i - \kappa_{i+3} a_{i+3} b_{i+1}(1-c_i) \end{aligned} \tag{2}$$

where $\kappa_i(\mathbf{r}, t)$ is a random Boolean variable which is 1 with probability k. The diffusion phase is a random reorganization of the particles along the direction of motion, followed by the displacement of the particles to a nearest neighbor,

$$a_i(\mathbf{r}+\mathbf{e}_i, t+1) = \sum_{l=0}^{3} \mu_l^{(a)} a_{i+l}'(\mathbf{r}, t) \tag{3}$$

where $\mathbf{e}_i$ are unit vectors pointing along the four main lattice directions. Similar equations hold for b_i and c_i. The quantities $\mu_l^{(a)}(\mathbf{r}, t)$ are the random Boolean variables responsible for the random motion.[24] It has been

shown[7] that the above microdynamics [Eqs. (2) and (3)] reproduces the usual reaction-diffusion equations when a mean-field approximation is introduced.

Nucleation and aggregation phenomena are implemented in our model according to general principles of supersaturation theory, but applied at a microscopic level. First, the C particles, once created, will diffuse until their local density (computed as the number of particles in a small neighborhood divided by its total number of sites and lattice directions) reaches a threshold value k_{sp}. Then they spontaneously precipitate and become D particles at rest (nucleation). We have considered 3×3 neighborhoods centered around each lattice site. Larger neighborhoods could possibly be envisaged, but they would have the tendency to average too much local density fluctuations.

Second, the C particles located in the vicinity of precipitate D particles will aggregate provided that their local density is larger than an aggregation threshold $k_p < k_{sp}$. Finally, a C particle sitting on the top of a D always becomes a D (a third threshold k could also be used here). The parameters k_p and k_{sp} are the two main control parameters of the model. The introduction of these critical values refers to the qualitative models of solidification theory, relating supersaturation and growth behavior.[14] From a microscopic point of view, it is common to describe the aggregation process in terms of a noise reduction algorithm[25]: C particles aggregate on a D cluster only after several encounters. The algorithm we use here is slightly different, but allows us to produce a fast enough aggregation process compared to the speed of the reaction front. A difference in these time scales is important for the formation of separate bands of precipitate.

Liesegang patterns are only obtained for a narrow range of parameters and a tedious tuning is necessary to produce them. In particular, it is important that the initial A concentration be significantly larger than the initial B concentration. In a cellular automata model with an exclusion principle, such a large difference implies having very few B particles. As a consequence, the production rate of C particles is quite low because very few reactions take place. For this reason, we have considered a pseudo-three-dimensional system composed of several two-dimensional layers. The reaction has been implemented so that particles of different layers can interact. However, such an approach is very demanding as far the computation time is concerned. Even on a massively parallel machine like an 8192 processor Connection Machine 2, the simulation of a system of size $512 \times 64 \times 64$ (Fig. 1a) takes about 10 hr to produce ten bands. In order to study systems with more bands, it is desirable to have a faster numerical scheme.

2.2. The Lattice Boltzmann Model

The outcome of a cellular automata simulation is generally very noisy, due to the discreteness of the state variables. Moreover, as we said, it offers little flexibility to adjust several parameters of the model. It may therefore be advantageous to simulate numerically directly the equations obtained by averaging and factorizing the cellular automata microdynamics. This implies that the many-body correlations are ignored. In this method, known as the lattice Boltzmann approach,[26] the Boolean variables entering into the cellular automata rules (2) and (3) are replaced by variables taking a continuous value in the interval [0, 1].

However, an important ingredient of the Liesegang pattern formation process is that spontaneous precipitation appears as a result of intrinsic local density fluctuations. Indeed, in the cellular automata model, nucleation occurs only at sites whose neighborhood contains at least $k_{sp}N$ particles. N is the product of the number of sites per neighborhood times the number of directions of motion (typically, for a 3×3 neighborhood, $N = 3^2 \times 4$). If, at a given site, the average particle density per direction is ρ, the probability that nucleation occurs is given by

$$p_{\text{nucl}}(\rho) = \sum_{l \geq k_{sp}N} \binom{N}{l} \rho^l (1-\rho)^{N-l} \tag{4}$$

A similar relation can be derived for the aggregation probability. Note that in this approach nucleation or aggregation may happen even if the average density is below the critical thresholds, so that the system may not be globally supersaturated.

In the Boltzmann approximation, due to the averaging process, these stochastic aspects are lost. In order to restore the effect of the fluctuations given by Eq. (4), one introduces a probabilistic component for the nucleation and aggregation processes. Nucleation and aggregation will take place only with given probabilities when the concentration reaches some renormalized threshold k_{sp} or k_p. The determination of these probabilities, as well as the new values of k_{sp} or k_p, can be done so as reproduce the behavior of (4).

From a qualitative point of view, the way the fluctuations are reintroduced does not play a crucial role. We have observed that if the A and B particles are injected randomly in the system, the effect of the local density variations is restored.

The lattice Boltzmann method allows us to gain a factor of 100 in the speed of the simulation and to produce up to 30 consecutive bands for systems of sizes 1024×64 (Fig. 1b).

2.3. The Model Without *C* Particles

The Prager–Zeldovitch model, in which no intermediate C particles are included, requires different rules for the solidification processes. On the other hand, the diffusion rule is identical. For the sake of numerical efficiency, we restrict ourselves to a lattice Boltzmann modeling.

In this scenario, the critical value k_{sp} corresponds to the value of the solubility product ab above which nucleation occurs according to the reaction $A + B \rightarrow AB$(solid). In the vicinity of precipitate, A and B will aggregate if $ab > k_p$; on the top of a precipitate particle, A and B aggregate provided that $ab > k$; k and k_p are such that $k < k_p < k_{sp}$. Finally, the depletion of A and B resulting from either nucleation or aggregation lowers the solubility product to the stationary or equilibrium-like value $ab = k$.

3. RESULTS OF THE SIMULATION FOR THE LIESEGANG BANDS

Figures 1a and 1b show typical examples of a cellular automata simulation with C particles giving rise to bands. From the positions x_n and the formation time t_n of each band we have verified[22] the spacing and the time laws. For instance, the plot given in Fig. 2 shows a very good agree-

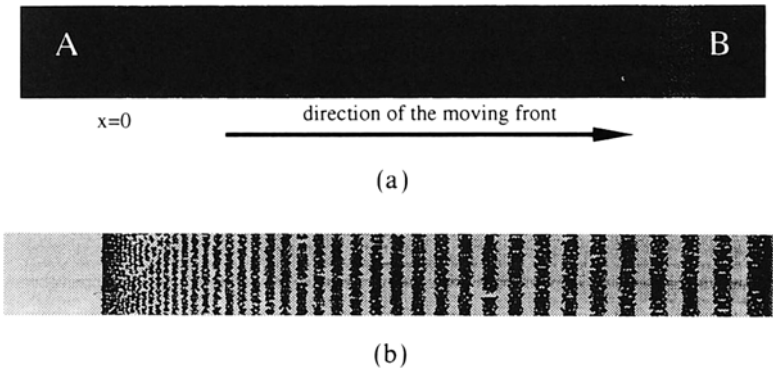

Fig. 1. (a) Formation of Liesegang bands in a test tube, as obtained from the cellular automata simulation of our model. The precipitate particles appear in separate bands as the reaction front moves from left to right. The particles produced from the A–B reaction (light grey domain before the letter B) indicate the position of the front at the time of this snapshot (after 18,000 iterations). The parameters of the simulation are $b_0/a_0 = 0.01$, $D_b/D_a = D_c/D_a = 0.1$, $k_{sp}/a_0 = 1.39 \times 10^{-2}$, and $k_p/a_0 = 6.07 \times 10^{-3}$. (b) Formation of Liesegang bands in a test tube, as obtained from the lattice Boltzmann simulation of our cellular automata model with C particles. The parameters of the simulation are $b_0/a_0 = 0.018$, $D_b/D_a = D_c/D_a = 0.1$, $k_{sp}/a_0 = 8.7 \times 10^{-3}$, and $k_p/a_0 = 6.5 \times 10^{-3}$.

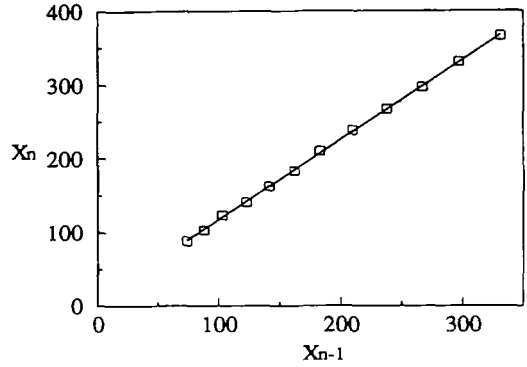

Fig. 2. Verification of the spacing law for the situation shown in Fig. 1. The slope gives $p = 1.08$.

ment for the relation $x_n/x_{n-1} \to p$. It is found that the so-called Jablczynski coefficient p is 1.08, a value well in the range of experimental findings. Indeed, the values obtained in different experiments with axial symmetries show that $1.05 \leqslant p \leqslant 1.20$. The way the value of p depends on the parameters of the model has not been investigated yet.

We also have studied[22] the way the width w_n of a band depends on its position. Whereas the time and spacing laws have been investigated in great detail in many experiments, much less seems to be known about a "width law." In most of the experiments, it is observed that w_n increases with x_n. A linear relation, derived from the width of only a few consecutive

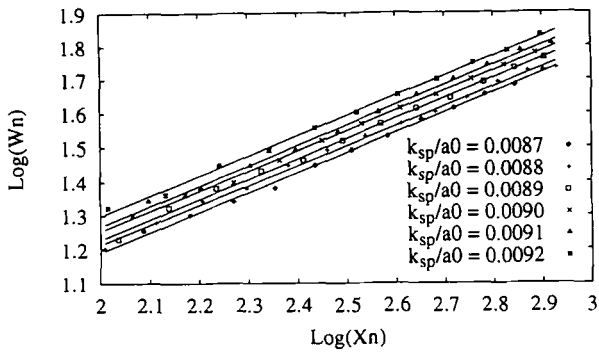

Fig. 3. Dependence of the width w_n of the Liesegang bands as a function of their position x_n, for various values of k_{sp}, for the concentration ratio $b_0/a_0 = 0.01$. We obtain $w_n = x_n^{0.59}$, independently of the value of k_{sp}.

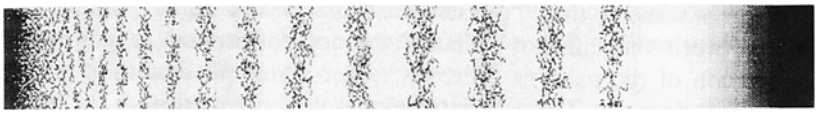

Fig. 4. Lattice Boltzmann simulation leading to Liesegang band formation in the model with no intermediate C particles. The precipitate AB(solid) is shown dark.

bands, has been proposed in the literature.[19, 27] Our simulations predict a more general relation

$$w_n \sim x_n^{\alpha} \tag{5}$$

where α is an exponent which depends on the initial concentrations a_0 and b_0. The width has been measured for the lattice Boltzmann simulations. It has been defined as the total spatial extension of a band. Although we cannot exclude for now the value $\alpha = 1$, we found for several simulations that α is typically in the range 0.5–0.6. (see Fig. 3).

The model without C particles (see Fig. 4) also exhibits the same features, showing that both scenarios are possible and that the interplay between a moving front and the rate of the precipitation-aggregation process is the key ingredient to the Liesegang pattern formation.

It is experimentally well known that Liesegang patterns are only found if the parameters of the experiment are thoroughly adjusted. Outside of the region where Liesegang patterns are formed, we have observed from our simulations that other types of patterns are obtained. These various patterns can be classified in a qualitative phase diagram, as shown in Fig. 5.

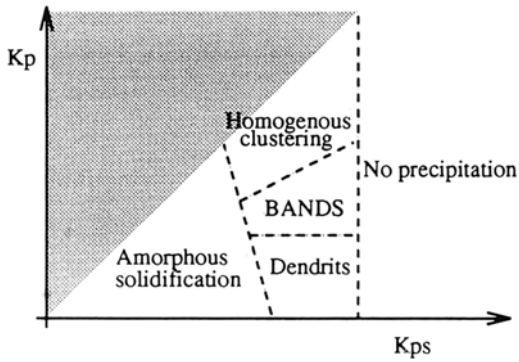

Fig. 5. Qualitative phase diagram showing the different possible patterns that can be obtained with our cellular automata model, as a function of the values of k_{sp} and k_p.

Examples of some of these "phases" are illustrated in Fig. 6. Note that the limits between the different "phases" do not correspond to any drastic modification of the patterns. There is rather a smooth crossover between the different domains. The associated names are borrowed from the phenomenological theory of solidification.[14, 28]

In real experiments, one cannot directly modify the parameters k_p and k_{sp}. However, it is experimentally possible to observe a crossover between different patterns by changing some properties of the gel (its pH,

(a)

(b)

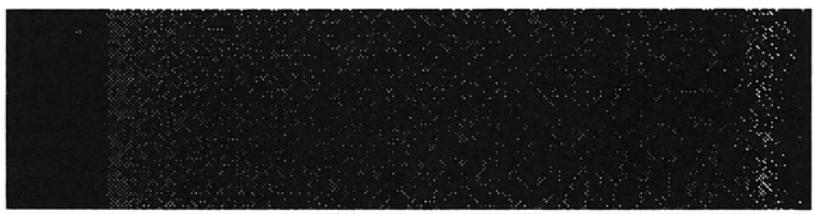

(c)

Fig. 6. Examples of patterns that are described in the phase diagram in Fig. 5. (a) Homogeneous clustering;[29] this is also the case of pattern (b), but closer to the region of band formation. (c) An example of what we called a dendrite structure.[28] Amorphous solidification would correspond to a completely uniform picture.

for example). These properties determine the diffusion-controlled aggregation processes from which one controls the level of supersaturation at the surface of growth (k_p).

4. TWO-DIMENSIONAL LIESEGANG RINGS AND SPIRALS

The formation of bands of precipitate in the simulations we have presented so far is an effect of the symmetry of the experiment (front moving along the x axis). The same model can be used in other situations as well, provided that the suitable boundary conditions are imposed during the simulation. An interesting case is the formation of rings or spirals[12] obtained when the reactant A is injected in the central region of a two-dimensional gel initially filled with B particles (cylindrical symmetry). The patterns shown in Fig. 7 are results of simulations of the lattice Boltzmann model with C particles. The size of the lattice is 1024×1024.

Figure 7a shows the situation where concentric rings of precipitate are formed in the wake of the reaction front. The parameters are $a_0 = 1$, $b_0/a_0 = 0.013$, $D_b/D_a = 0.1$, $k_{sp}/a_0 = 0.0087$, and $k_p/a_0 = 0.0065$. The nucleation process takes place with a probability of 0.05 and aggregation with a probability close to 1. Similar rings are also obtained within the model without C particles.

For the same set of parameters but $b_0/a_0 = 0.016$, a different pattern occurs as shown on Fig. 7b. Here, a local defect produced by a density fluctuation develops and a spiral of precipitate appears instead of rings. Such a spiral pattern will never be obtained from a deterministic model which does not allows local density fluctuations.

From our data, we have checked the validity of the spacing law for ring formation. The relation

$$r_n/r_{n-1} \to p \tag{6}$$

where r_n is the radius of the nth ring, is also observed. In Fig. 8, the Jablczynski coefficient p is plotted as a function of the concentration of B particles b_0 (for $a_0 = 1$) both for axial (bands) and cylindrical (rings) symmetries. One notices that p decreases when b_0 increases, in agreement with experimental data. Moreover, for the same set of parameters, the value of p is found to be larger in the case of rings than it is for bands. This could be checked experimentally.

5. CONCLUSIONS

We have shown that our cellular automata approach for the formation of Liesegang patterns is able to reproduce many aspects experimentally

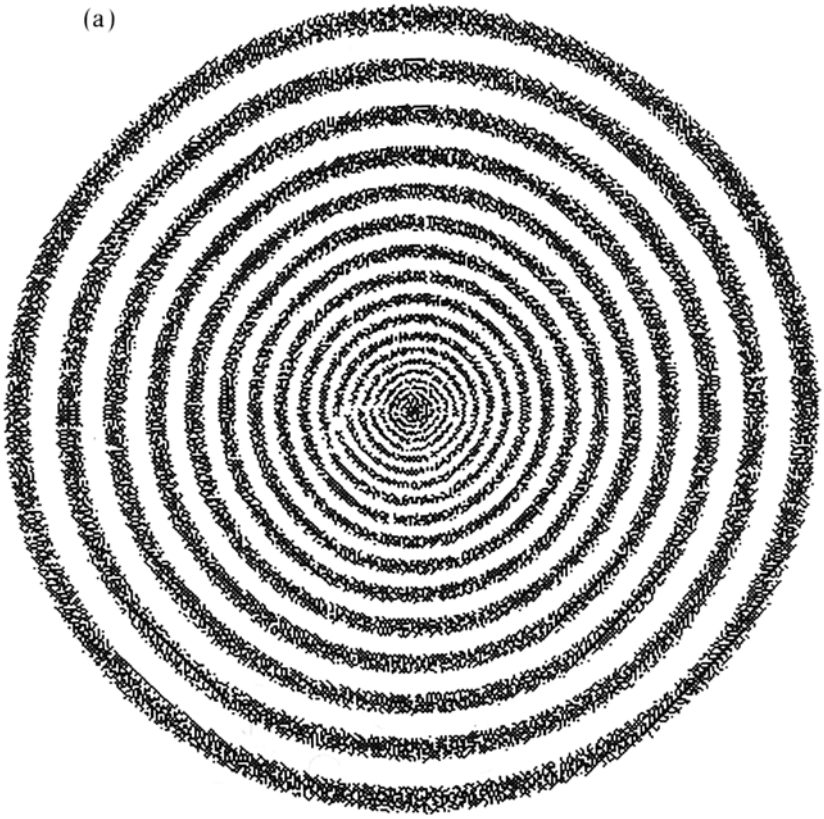

Fig. 7. Formation of (a) Liesegang rings and (b) spirals, as obtained after 2000 iterations of the lattice Boltzmann model with C particles.

observed. In addition, it offers new predictions and a description of the microscopic structure of the bands. The basic mechanisms we have incorporated in the dynamics are simple and quite natural, at a microscopic level. The key idea is a microscopic supersaturation hypothesis.

Fluctuations are included in the description and play a crucial role in the solidification process. Spontaneous precipitation (homogeneous nucleation) and aggregation phenomena are driven by these local denisty fluctuations. The statistical variations of the number of particles in a small volume element produce random nucleation centers in a region where the density is close to the supersaturation threshold. Similarly, fluctuations make the situation locally favorable for aggregation to take place when the average density is large enough. These features are naturally taken into account in

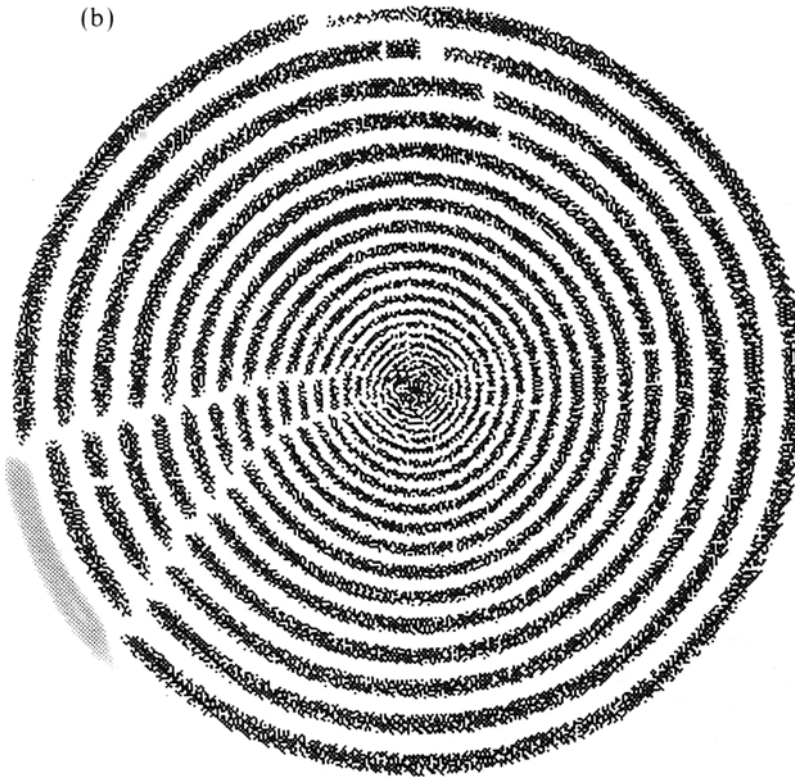

Fig. 7. (*Continued*)

the cellular automata approach because particles are actually present in the model.

Spontaneous fluctuations are lost in the lattice Boltzmann models, due to the averaging process. The simple arguments of Section 2.2 show that local fluctuations result in nucleation and aggregation probabilities which are functions of the density and the saturation thresholds [see Eq. (4)]. The same effect can be restored in a lattice Boltzmann dynamics by also adding a constant probability of nucleation and aggregation when the local density reaches some renormalized threshold values k_p and k_{sp}. This is a crude but effective approximation of relation (4) (and the corresponding one for aggregation). The average nucleation and growth rates of our models follow from these probabilities and can be compared with the usual relations found in the literature.[19, 20]

It is interesting to note that, due to the presence of these intrinsic

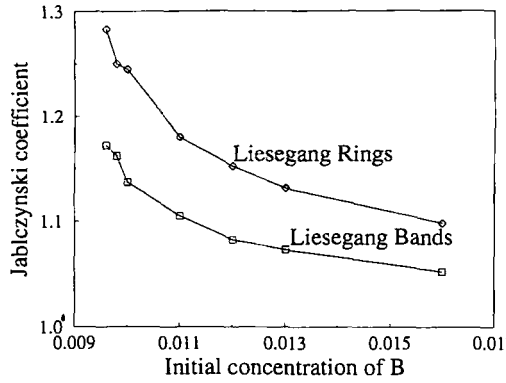

Fig. 8. Jablczynski coefficient p as a function of the concentration b_0 of B particles (for $a_0 = 1$), for both axial (bands) and cylindrical (rings) symmetries.

fluctuations in our models, there is no need to distinguish between what are usually called structures with and without initial concentration gradient.[20] Both follow from the same microscopic supersaturation mechanism. Band formation results from a reaction-diffusion front initiated by a macroscopic gradient concentration, whereas homogeneous growth takes place in directions where no macroscopic gradient exists.

The spontaneous fluctuations in the cellular automata description and the noise added in the lattice Boltzmann approach break the symmetry of the experiment. First, in the case of bands, one sees a structure in the direction perpendicular to the motion of the front. This would be out of reach of a traditional approach. Second, in the case of rings, our models also lead to spirals, as observed experimentally. This is a manifestation of a large local fluctuation which causes a structure defect.

An interesting extension of the present work would be to include a redissolution mechanism for the particles in a solid cluster. New ingredients, such as a variation of the diffusion coefficients, could be considered in order to investigate the capability of our approach to model inverse banding, as suggested in ref. 15.

ACKNOWLEDGMENT

We would like to dedicate this paper to Philippe Choquard, who early recognized the importance of numerical simulations in statistical physics.

REFERENCES

1. M. Bramson and J. Lebowitz, *J. Stat. Phys.* **62**:297 (1991).
2. S. Cornell, M. Droz, and B. Chopard, *Physica A* **188**:322 (1992).
3. S. Cornell, M. Droz, and B. Chopard, *Phys. Rev. A* **44**:4826 (1991).
4. S. Cornell and M. Droz, *Phys. Rev. Lett.* **70**:3824 (1993).
5. Nonequilibrium Chemical Dynamics: From Experiment to Microscopic Simulations, *Physica* **188**:1–468 (1992).
6. M. Droz and L. Frachebourg, *Helv. Phys. Acta* **66**:97 (1993).
7. B. Chopard, S. Cornell, M. Droz, and L. Frachebourg, in *Cellular Automata: Prospects in Astrophysical Applications*, J. M. Perdang and A. Lejeune, eds. (World Scientific, Singapore, 1993), pp. 157–186.
8. D. Dab, J.-P. Boon, and Y.-X. Li, *Phys. Rev. Lett.* **66**:2535 (1991).
9. R. Kapral, A. Lawniczak, and P. Masiar, *Phys. Rev. Lett.* **66**:2539 (1991).
10. K. Jablczynski, *Bull. Soc. Chim. Fr.* **33**:1592 (1923).
11. R. E. Liesegang, *Naturwiss. Wochenschr.* **11**:353 (1896).
12. R. E. Liesegang, *Photog. Arch.* **21**:221 (1896).
13. L. Gálfi and Z. Rácz, *Phys. Rev. A* **38**:3151 (1988).
14. H. K. Henisch, *Periodic Precipitation* (Pergamon Press, 1991).
15. B. Mathur and S. Ghosh, *Kolloid-Z.* **159**:143 (1958).
16. S. Prager, *J. Chem. Phys.* **25**:279 (1956).
17. Ya. B. Zeldovitch, G. I. Barrenblatt, and R. L. Salganik, *Sov. Phys. Dokl.* **6**:869 (1962).
18. D. A. Smith, *J. Phys. Chem.* **81**:3102 (1984).
19. G. T. Dee, *Phys. Rev. Lett.* **57**:275 (1986).
20. M. E. Le Van and J. Ross, *J. Phys. Chem.* **91**:6300 (1987).
21. W. Ostwald, *Lehrbuch der allgemeinen Chemie* (Engelman, Leipzig, 1897).
22. B. Chopard, P. Luthi, and M. Droz, *Phys. Rev. Lett.* **72**:1384 (1994).
23. T. A. Witten, in *On Growth and Form*, H. E. Stanley and N. Ostrowsky, eds. (Martinus Nijhoff, 1985), p. 54.
24. B. Chopard and M. Droz, *J. Stat. Phys.* **64**:859 (1991).
25. J. Nittmann and H. E. Stanley, *J. Phys. A* **20**:L1185 (1987).
26. R. Benzi, S. Succi, and M. Vergassola, *Physics Reports* **222**:145 (1992).
27. K. M. Pillai, V. K. Vaidyan, and M. A. Ittyachan, *Colloid Polymer Sci.* **258**:831 (1980).
28. B. Chopard, H. J. Herrmann, and T. Vicsek, *Nature* **353**:409 (1991).
29. I. Sunagawa, *Bull. Mineral.* **104**:81 (1981).